

Evaluating Soil Liquefaction and Post-earthquake deformations using the CPT

P.K. Robertson

University of Alberta, Dept. of Civil and Environmental Engineering, Edmonton, Canada

Keywords: Soil liquefaction, ground deformations, site investigation, cone penetration test.

ABSTRACT: Soil liquefaction is a major concern for many structures constructed with or on sand or sandy soils. This paper provides an overview of soil liquefaction, describes a method to evaluate the potential for cyclic liquefaction using the Cone Penetration Test (CPT) and methods to estimate post-earthquake ground deformations. A discussion is also provided on how to estimate the liquefied undrained shear strength following strain softening (flow liquefaction).

1 INTRODUCTION

Soil liquefaction is a major concern for structures constructed with or on sand or sandy soils. The major earthquakes of Niigata in 1964 and Kobe in 1995 have illustrated the significance and extent of damage caused by soil liquefaction. Soil liquefaction is also a major design problem for large sand structures such as mine tailings impoundment and earth dams.

To evaluate the potential for soil liquefaction it is important to determine the soil stratigraphy and in-situ state of the deposits. The CPT is an ideal in-situ test to evaluate the potential for soil liquefaction because of its repeatability, reliability, continuous data and cost effectiveness. This paper presents a summary of the application of the CPT to evaluate soil liquefaction. Further details are contained in a series of papers (Robertson and Wride, 1998; Youd et al., 2001; Zhang et al., 2002; Zhang et al., 2004).

2 DEFINITION OF SOIL LIQUEFACTION

Several phenomena are described as soil liquefaction, hence, a series of definitions are provided to aid in the understanding of the phenomena.

2.1 Cyclic (softening) Liquefaction

- Requires undrained cyclic loading during which shear stress reversal occurs or zero shear stress can develop.
- Requires sufficient undrained cyclic loading to allow effective stresses to reach essentially zero.
- Deformations during cyclic loading can accumulate to large values, but generally stabilize shortly after cyclic loading stops. The resulting movements are due to external causes and occur mainly during the cyclic loading.
- Can occur in almost all saturated sandy soils provided that the cyclic loading is sufficiently large in magnitude and duration.
- Clayey soils generally do not experience cyclic liquefaction and deformations are generally small due to the cohesive nature of the soils. Rate effects (creep) often control deformations in cohesive soils.

2.2 Flow Liquefaction

- Applies to strain softening soils only.
- Requires a strain softening response in undrained loading resulting in approximately constant shear stress and effective stress.
- Requires in-situ shear stresses to be greater than the residual or minimum undrained shear strength

- Either monotonic or cyclic loading can trigger flow liquefaction.
- For failure of a soil structure to occur, such as a slope, a sufficient volume of material must strain soften. The resulting failure can be a slide or a flow depending on the material characteristics and ground geometry. The resulting movements are due to internal causes and can occur after the trigger mechanism occurs.
- Can occur in any metastable saturated soil, such as very loose fine cohesionless deposits, very sensitive clays, and loess (silt) deposits.

Note that strain softening soils can also experience cyclic liquefaction depending on ground geometry. Figure 1 presents a flow chart (Robertson and Wride, 1998) to clarify the phenomena of soil liquefaction.

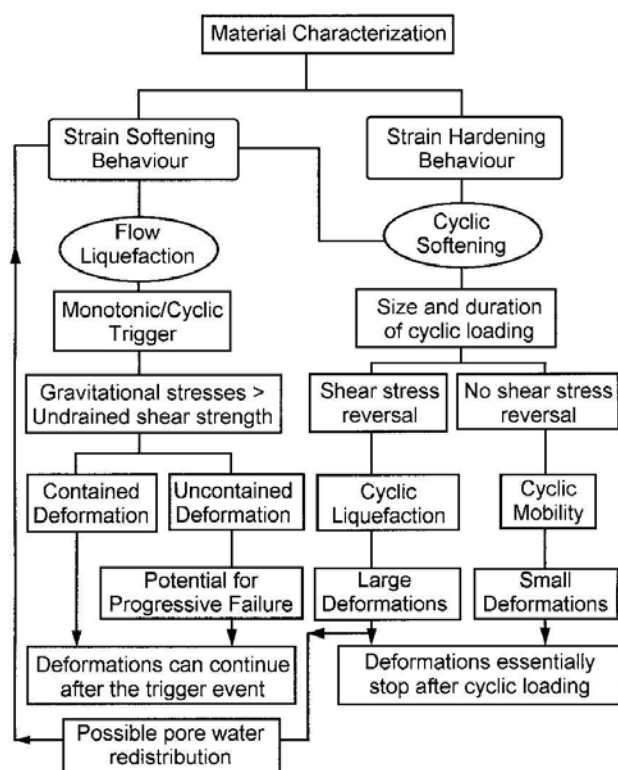


Figure 1. Flow chart to evaluate liquefaction of soils (After Robertson and Wride, 1998)

If a soil is strain softening, flow liquefaction is possible if the soil can be triggered to collapse and if the gravitational shear stresses are larger than the minimum undrained shear strength. The trigger can be either monotonic or cyclic. Whether a slope or soil structure will fail and slide will depend on the amount of strain softening soil relative to strain hardening soil within the structure, the brittleness of the strain softening soil and the geometry of the ground. The resulting deformations of a soil structure with both strain softening and strain hardening soils will depend on many factors,

such as distribution of soils, ground geometry, amount and type of trigger mechanism, brittleness of the strain softening soil and drainage conditions. Examples of flow liquefaction failures are the Aberfan flow slide (Bishop, 1973), Zealand submarine flow slides (Koppejan et al., 1948) and the Stava tailings dam failure. In general, flow liquefaction failures are not common, however, when they occur, they typically take place rapidly with little warning and are usually catastrophic. Hence, the design against flow liquefaction should be carried out cautiously.

If a soil is strain hardening, flow liquefaction will not occur. However, cyclic liquefaction can occur due to cyclic undrained loading. The amount and extent of deformations during cyclic loading will depend on the density of the soils, the magnitude and duration of the cyclic loading and the extent to which shear stress reversal occurs. If extensive shear stress reversal occurs and the magnitude and duration of the cyclic loading are sufficiently large, it is possible for the effective stresses to essentially reach zero with resulting possible large deformations. Examples of cyclic liquefaction were common in the major earthquakes in Niigata in 1964 and Kobe in 1995 and manifest in the form of sand boils, damaged lifelines (pipelines, etc.) lateral spreads, slumping of embankments, ground settlements, and ground surface cracks. If cyclic liquefaction occurs and drainage paths are restricted due to overlying less permeable layers, the sand immediately beneath the less permeable soil can loosen due to pore water redistribution, resulting in possible subsequent flow liquefaction, given the right geometry.

The three main concerns related to soil liquefaction are generally:

- Will an event (e.g. a design earthquake) trigger significant zones of liquefaction?
- What displacements will result, if liquefaction is triggered?
- What will be the resulting residual (minimum) undrained shear strength, if a soil is potentially strain softening (and is triggered to liquefy)?

This paper describes how the CPT can be used to evaluate the potential for an earthquake to trigger cyclic liquefaction, and, then how to estimate post-earthquake displacements (vertical and lateral). Finally, a method is described on how to estimate the minimum undrained shear strength, using the CPT, which could result if the soil is potentially strain softening (flow liquefaction).

3 CYCLIC LIQUEFACTION

Most of the existing work on cyclic liquefaction has been primarily for earthquakes. The late Prof. H.B. Seed and his co-workers developed a comprehensive methodology to estimate the potential for cyclic liquefaction due to earthquake loading. The methodology requires an estimate of the cyclic stress ratio (CSR) profile caused by the design earthquake and the cyclic resistance ratio (CRR) of the ground. If the CSR is greater than the CRR cyclic liquefaction can occur. The CSR is usually estimated based on a probability of occurrence for a given earthquake. A site-specific seismicity analysis can be carried out to determine the design CSR profile with depth. A simplified method to estimate CSR was also developed by Seed and Idriss (1971) based on the maximum ground surface acceleration (a_{max}) at the site. The simplified approach can be summarized as follows:

$$CSR = \frac{\tau_{av}}{\sigma'_{vo}} = 0.65 \left[\frac{a_{max}}{g} \right] \left(\frac{\sigma_{vo}}{\sigma'_{vo}} \right) r_d \quad [1]$$

Where τ_{av} is the average cyclic shear stress; a_{max} is the maximum horizontal acceleration at the ground surface; $g = 9.81m/s^2$ is the acceleration due to gravity; σ_{vo} and σ'_{vo} are the total and effective vertical overburden stresses, respectively; and r_d is a stress reduction factor which is dependent on depth. The factor r_d can be estimating using the following bi-linear function, which provides a good fit to the average of the suggested range in r_d originally proposed by Seed and Idriss (1971):

$$r_d = 1.0 - 0.00765z \quad [2]$$

if $z < 9.15$ m

$$= 1.174 - 0.0267z$$

if $z = 9.15$ to 23 m

Where z is the depth in metres. These formulae are approximate at best and represent only average values since r_d shows considerable variation with depth.

Seed et al., (1985) also developed a method to estimate the cyclic resistance ratio (CRR) for clean sand with level ground conditions based on the Standard Penetration Test (SPT). Recently the CPT has become more popular to estimate CRR, due to the continuous, reliable and repeatable nature of the data (Youd et al., 2001).

In recent years, there has been an increase in available field performance data, especially for the CPT (Robertson and Wride, 1998). The recent field performance data have shown that the existing CPT-based correlation by Robertson and Campanella (1985) for clean sands is generally good. Based on discussions at the 1996 NCEER workshop (NCEER, 1997), the curve by Robertson and Campanella (1985) has been adjusted slightly at the lower end. The resulting recommended CPT correlation for clean sand is shown in Figure 2 and can be estimated using the following simplified equations:

$$CRR_{7.5} = 93 \left[\frac{(q_{c1N})_{cs}}{1000} \right]^3 + 0.08 \quad [3]$$

if $50 \leq (q_{c1N})_{cs} \leq 160$

$$CRR_{7.5} = 0.833 \left[\frac{(q_{c1N})_{cs}}{1000} \right] + 0.05$$

if $(q_{c1N})_{cs} < 50$

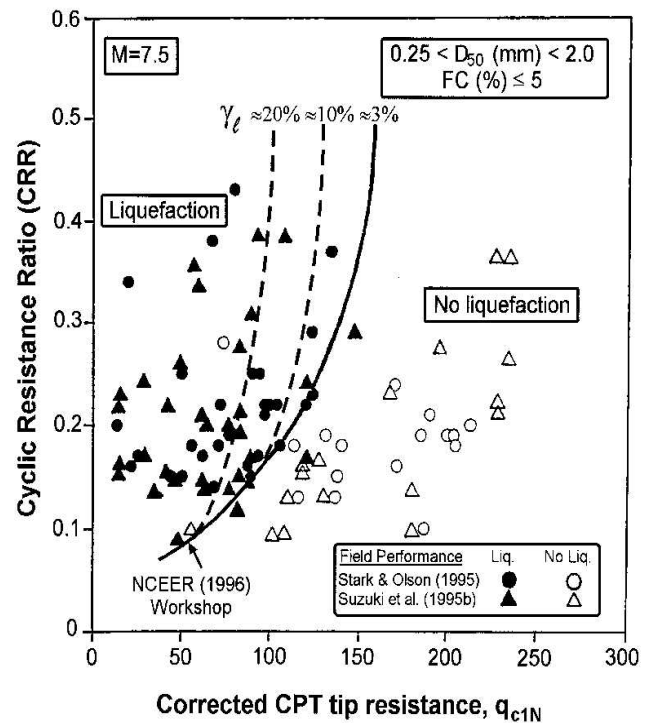


Figure 2. Cyclic resistance ratio (CRR) from the CPT for clean sands. (After Robertson and Wride, 1998).

Where $(q_{c1N})_{cs}$ is the equivalent clean sand normalized cone penetration resistance (defined in detail later).

The field observations used to compile the curve in Figure 2 are based primarily on the following conditions:

- Holocene age, clean sand deposits
- Level or gently sloping ground
- Magnitude $M = 7.5$ earthquakes
- Depth range from 1 to 15 m (85% is for depths < 10 m)
- Representative average CPT values for the layer considered to have experienced cyclic liquefaction.

Caution should be exercised when extrapolating the CPT correlation to conditions outside the above range. An important feature to recognize is that the correlation is based primarily on average values for the inferred liquefied layers. However, the correlation is often applied to all measured CPT values, which include low values below the average. Therefore, the correlation can be conservative in variable deposits where a small part of the CPT data can indicate possible liquefaction.

It has been recognized for some time that the correlation to estimate $CRR_{7.5}$ for silty sands is different than that for clean sands. Typically a correction is made to determine an equivalent clean sand penetration resistance based on grain characteristics, such as fines content, although the corrections are due to more than just fines content, since the plasticity of the fines also has an influence on the CRR.

One reason for the continued use of the SPT has been the need to obtain a soil sample to determine the fines content of the soil. However, this has been offset by the generally poor repeatability and reliability of the SPT data. It is now possible to estimate grain characteristics directly from the CPT. Robertson and Wride (1998) suggest estimating an equivalent clean sand normalized cone penetration resistance, $(q_{c1N})_{cs}$ using the following:

$$(q_{c1N})_{cs} = K_c (q_{c1N}) \quad [4]$$

where K_c is a correction factor that is a function of grain characteristics of the soil.

Robertson and Wride (1998) suggest estimating the grain characteristics using the soil behavior chart by Robertson (1990) (see Figure 3) and the soil behavior type index, I_c , where;

$$I_c = \left[(3.47 - \log Q)^2 + (\log F + 1.22)^2 \right]^{0.5} \quad [5]$$

$$\text{where } Q = q_{c1N} = \left(\frac{q_c - \sigma_{vo}}{P_{a2}} \right) \left(\frac{P_a}{\sigma'_{vo}} \right)^n$$

is the normalized CPT penetration resistance, dimensionless; n = stress exponent; $F = f_s / [(q_c - \sigma_{vo})] \times 100\%$ is the normalized friction ratio, in percent; f_s is the CPT sleeve friction stress; σ_{vo} and σ'_{vo} are the total effective overburden stresses, respectively; P_a is a reference pressure in the same units as σ'_{vo} (i.e. $P_a = 100$ kPa if σ'_{vo} is in kPa); and P_{a2} is a reference pressure in the same units as q_c and σ_{vo} (i.e. $P_{a2} = 0.1$ MPa if q_c and σ_{vo} are in MPa). Robertson and Wride (1998) used a form of q_{c1N} that did not subtract the total vertical stress (σ_{vo}) from q_c and used $n = 0.5$. The more correct approach is the full form shown in equation 5. In general there is little difference between q_{c1N} and Q for most sandy soils at shallow depth ($\sigma'_{vo} < 300$ kPa).

The soil behaviour type chart by Robertson (1990) shown in Figure 3, uses a normalized cone penetration resistance (Q) based on a simple linear stress exponent of $n = 1.0$, whereas the chart recommended here for estimating CRR in sand is based on a normalized cone penetration resistance (q_{c1N}) based on a stress exponent $n = 0.5$.

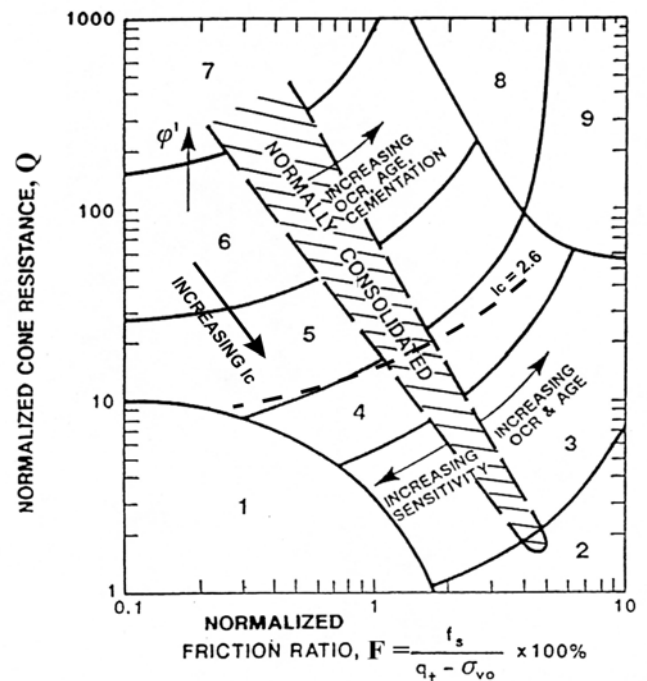


Figure 3. Normalized CPT soil behaviour type chart. (After Robertson, 1990).

Olsen and Malone (1988) correctly suggested a normalization where the stress exponent (n) varies from around 0.5 in sands to 1.0 in clays. The procedure using $n = 1.0$ was recommended by Robertson and Wride (1998) for soil classification in clay type soils when $I_c > 2.6$. However, in sandy soils when $I_c \leq 2.6$, Robertson and Wride (1998) recommended that data being plotted on the chart be modified by using $n = 0.5$.

Zone	Soil Behaviour Type	I_c
1	Sensitive, fine grained	N/A
2	Organic soils – peats	> 3.6
3	Clays – silty clay to clay	2.95 - 3.6
4	Silt mixtures – clayey silt to silty clay	2.60 – 2.95
5	Sand mixtures – silty sand to sandy silt	2.05 – 2.6
6	Sands – clean sand to silty sand	1.31 – 2.05
7	Gravelly sand to dense sand	< 1.31
8	Very stiff sand to clayey sand*	N/A
9	Very stiff, fine grained*	N/A

* Heavily overconsolidated or cemented

Note: Soil behaviour type index (I_c) is given by

$$I_c = [(3.47 - \log Q)^2 + (\log F + 1.22)^2]^{0.5}$$

The simplified normalization suggested by Robertson and Wride (1998) is easy to apply but produces a somewhat discontinuous variation of the stress exponent, n . To produce a smoother variation of the stress exponent the following modified method is recommended.

Assume an initial stress exponent $n = 1.0$ and calculate Q and F and then I_c . Then:

$$\text{If } I_c < 1.64 \quad n = 0.5 \quad [6]$$

$$\text{If } I_c > 3.30 \quad n = 1.0$$

$$\text{If } 1.64 < I_c < 3.30 \quad n = (I_c - 1.64) 0.3 + 0.5$$

Iterate until the change in the stress exponent, $\Delta n < 0.01$.

When the in-situ vertical effective stress (σ'_{vo}) exceeds 300 kPa assume $n = 1.0$ for all soils. This avoids the need to make further corrections for high overburden stresses (i.e. K_σ).

The recommended relationship between I_c and the correction factor K_c is given by the following:

$$K_c = 1.0 \text{ if } I_c \leq 1.64 \quad [7]$$

$$K_c = -0.403 I_c^4 + 5.581 I_c^3 - 21.63 I_c^2 + 33.75 I_c - 17.88 \text{ if } I_c > 1.64$$

The correction factor, K_c , is approximate since the CPT responds to many factors, such as, soil plasticity, fines content, mineralogy, soil sensitivity, age and stress history. However, in general, these same factors influence the $CRR_{7.5}$ in a similar manner. Caution should be used when applying the relationship to sands that plot in the region de-

finied by $1.64 < I_c < 2.36$ and $F < 0.5\%$ so as not to confuse very loose clean sands with sands containing fines. In this zone, it is suggested to set $K_c = 1.0$, to provide some added conservatism.

Soils with $I_c > 2.6$ fall into the clayey silt, silty clay and clay regions of the CPT soil behavior chart and, in general, are essentially non-liquefiable in terms of cyclic liquefaction. Samples should be obtained and liquefaction evaluated using other criteria based on index parameters (Youd et al., 2001). Soils that fall in the lower left region of the CPT soil behavior chart defined by $I_c > 2.6$ but $F < 1.0\%$ can be sensitive fine-grained soils and hence, possibly susceptible to both cyclic and flow liquefaction. Fine-grained, cohesive (clay) soils can develop significant strains and deformations during earthquake loading if the level and duration of shaking are sufficient to overcome the peak undrained resistance of the soil. If that were to happen and sufficient movement were to accrue, the strength of the soil could reduce to its residual or remolded strength depending on the amount of strain required to soften the soil.

The full methodology to estimate $CRR_{7.5}$ from the CPT is summarized in Figure 4.

Recent publications have attempted to update the relationship between normalized cone resistance (q_{cIN}) and CRR (Figure 2). However, these efforts have limited additional value since the relationship is based on average values in layers that were thought to have liquefied. This requires considerable judgment and is subject to much uncertainty. It is now time to move away from the boundary curve diagrams represented in Figure 2. The preferred approach is to continue to refine the total integrated CPT-based approach based on case histories using the full CPT and CRR profiles. Ideally case histories should include extensive CPT data, samples and observations of ground deformations (both surface and subsurface) so that a full evaluation can be made of the impact of the earthquake loading and where the deformations occurred. This can be important, since deformations can occur where full liquefaction may not have taken place (i.e. factor of safety greater than 1). Currently most publications take case history data and estimate the layer that experienced liquefaction and then assign an average penetration resistance value to that layer. In this way each case history can be represented by one data point. However, each case history should be represented by the many hundred data points contained in the full CPT profile. Often the ground profiles are complex and liquefaction may not have occurred in one well-defined single layer.

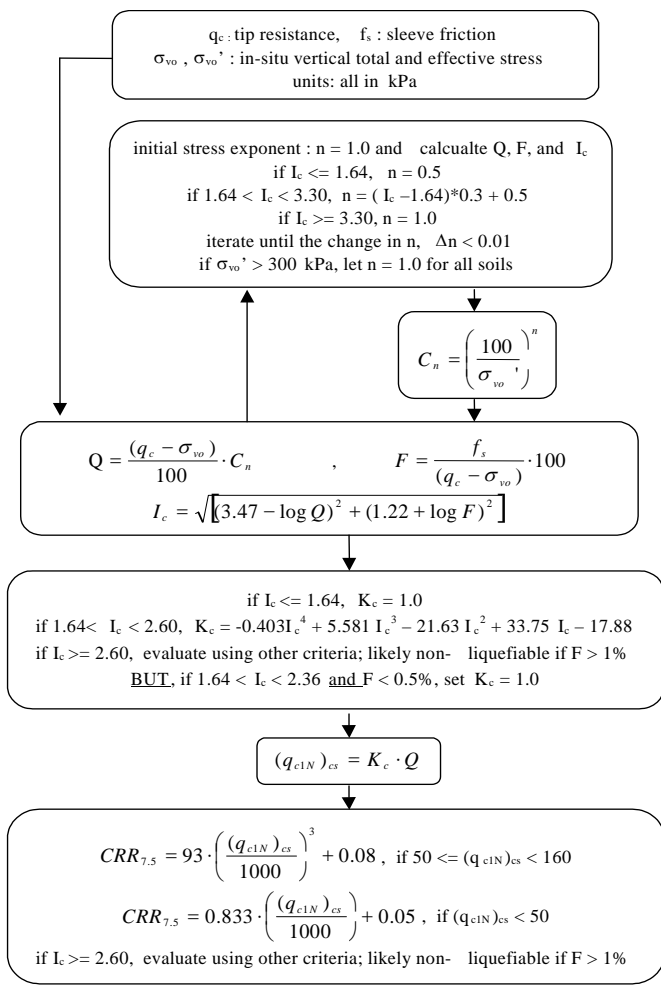


Figure 4. Flow chart to evaluate cyclic resistance ratio (CRR) from the CPT. (Modified from Robertson and Wride, 1998).

Liquefaction often occurs in multiple layers, which can only be observed in the full CPT profile. It can be overly simplistic to represent a complex ground profile and case history by one data point on a boundary curve like Figure 2. These curves have served as an excellent starting point in the development of the current simplified CPT and SPT liquefaction methods now available, however, it is now time to leave these highly simplistic curves and progress using data captured in the full soil profile.

The factor of safety against liquefaction is defined as:

$$\text{Factor of Safety, FS} = \frac{CRR_{7.5}}{CSR} \cdot MSF \quad [8]$$

where MSF is the Magnitude Scaling Factor to convert the $CRR_{7.5}$ for $M = 7.5$ to the equivalent CRR for the design earthquake. The recommended MSF is given by:

$$MSF = \frac{174}{M^{2.56}} \quad [9]$$

The above recommendations are based on the NCEER Workshop in 1996 (Youd et al., 2001).

An example of the CPT method to evaluate cyclic liquefaction is shown on Figure 5 for the Moss Landing site that suffered cyclic liquefaction during the 1989 Loma Prieta earthquake in California (Boulanger et al., 1997).

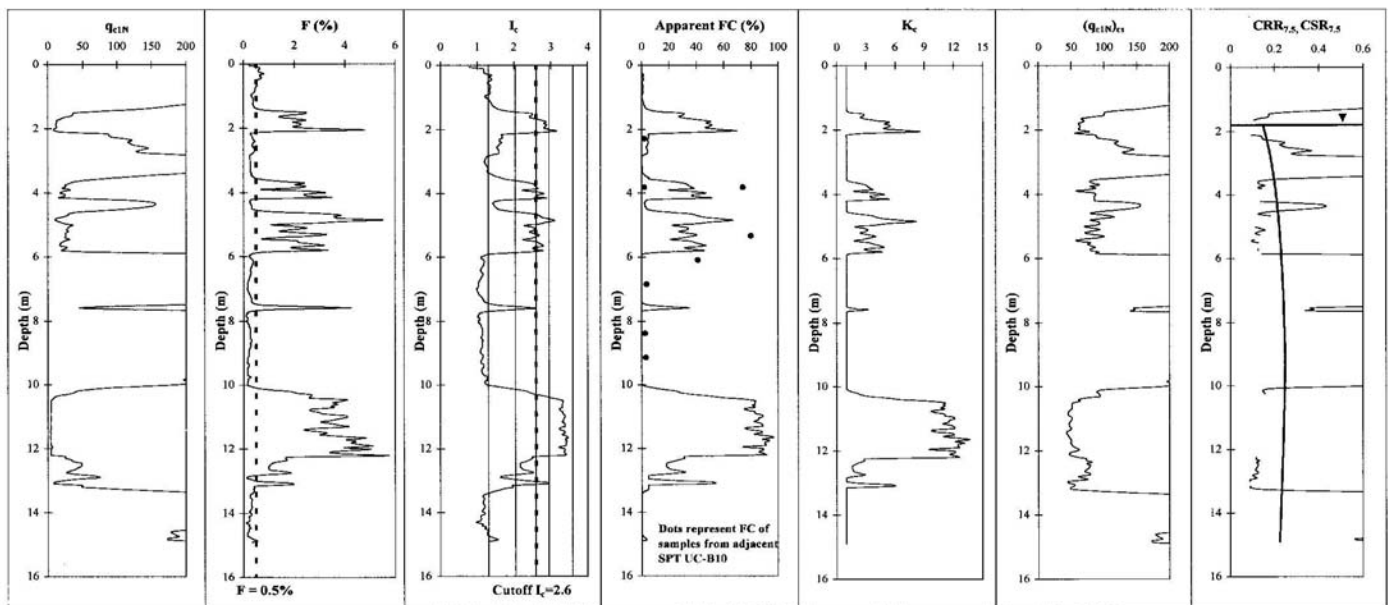


Figure 5. Example of CPT to evaluate cyclic liquefaction at Moss Landing Site. (After Robertson and Wride, 1998).

A major advantage of the CPT approach is the continuous and reliable nature of the data. CPT data are typically collected every 5 cm (2 inches). This means that data points are collected at the interface between layers, such as between clay and sand. During this transition, the CPT data points do not accurately capture the correct soil response since the penetration resistance is moving from either low to high values or vis-a-versa. The CPT penetration resistance represents an average response of the ground within a sphere of influence that can vary from a few cone diameters in soft clay to 20 cone diameters in dense sand. In these thin transition zones the CPT-based liquefaction method can predict low values of CRR. This is illustrated in Figure 5 at depths of around 6m and 10m, where there are clear interface boundaries between sand and clay. At these locations there are a few data points that indicate low values of CRR and hence liquefaction. These thin interface zones are easy to identify and account for in the interpretation. In the following sections, methods to estimate post-earthquake ground deformations will be presented and discussed. Using these CPT-based methods, it is simple to identify the thin interface transition zones and remove, where appropriate.

A key advantage of the CPT based liquefaction method is that continuous profiles can be calculated quickly, which allows the engineer time to study the profile in detail and apply engineering judgment where appropriate. The CPT-based liquefaction method is a simplified approach and is hence conservative. The method was developed from the limit boundary curve in Figure 2 that was developed using average values but the resulting method is applied using all data points. Also, the continuous CPT data predicts low values of CRR in the thin interface transition zones, as described above.

Juang et al. (1999) has shown that the Robertson and Wride CPT-based liquefaction method has the same level of conservatism as the Seed et al SPT-based liquefaction method, both represent a probability of liquefaction of between 20% to 30% (i.e. more conservative than the expected 50% probability). This conclusion was supported by the NCEER workshop (Youd et al., 2001).

4 POST-EARTHQUAKE DEFORMATIONS

The CPT-based method described above, can provide continuous profiles of CRR and Factor of Safety for given design earthquake loading. However, Factor of Safety is not always the most mean-

ingful means to evaluate liquefaction potential. For most projects a more meaningful evaluation of the effect of a design earthquake on a given project is to estimate the ground deformations that may result from the earthquake. Ground deformations that follow earthquake loading are either vertical settlements or lateral deformations. Although the Factor of Safety due to a design earthquake may be less than 1.0, the resulting deformations may be either acceptable for the project or can be accommodated with appropriate design of the structures.

5 LIQUEFACTION INDUCED VERTICAL GROUND SETTLEMENTS

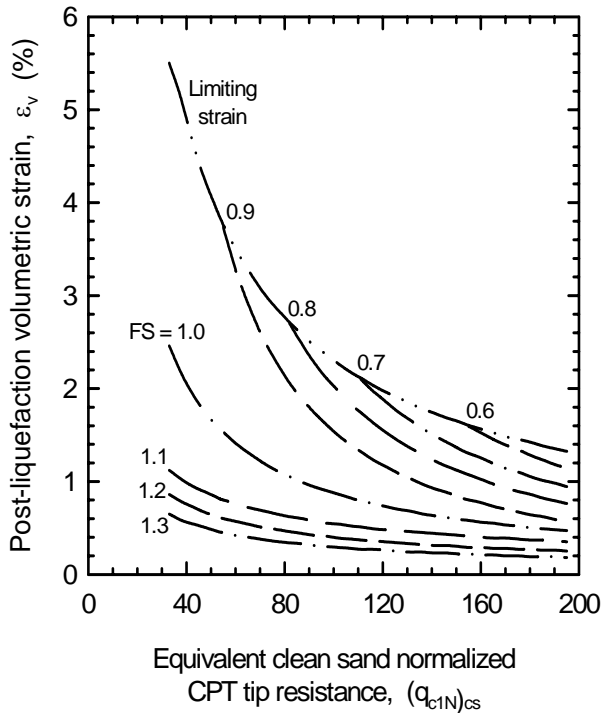
Liquefaction-induced ground settlements are essentially vertical deformations of surficial soil layers caused by the densification and compaction of loose granular soils following earthquake loading. Several methods have been proposed to calculate liquefaction-induced ground deformations, including numerical and analytical methods, laboratory modeling and testing, and field-testing-based methods. The expense and difficulty associated with obtaining and testing high quality samples of loose sandy soils may only be feasible for high-risk projects where the consequences of liquefaction may result in severe damage and large costs. Semi-empirical approaches using data from field tests are likely best suited to provide simple, reliable and direct methods to estimate liquefaction-induced ground deformations for low to medium risk projects, and also to provide preliminary estimates for higher risk projects. Zhang et al. (2002) proposed a simple semi-empirical method using the CPT to estimate liquefaction induced ground settlements for level ground.

For sites with level ground, far from any free face (e.g., river banks, seawalls), it is reasonable to assume that little or no lateral displacement occurs after the earthquake, such that the volumetric strain will be equal or close to the vertical strain. If the vertical strain in each soil layer is integrated with depth using Equation [10], the result should be an appropriate index of potential liquefaction-induced ground settlement at the CPT location due to the design earthquake,

$$S = \sum_{i=1}^j \varepsilon_{vi} \Delta z_i \quad [10]$$

Where: S is the calculated liquefaction-induced ground settlement at the CPT location; ε_{vi} is the post-liquefaction volumetric strain for the soil sub-layer i ; Δz_i is the thickness of the sub-layer i ; and j is the number of soil sub-layers.

The method suggested by Zhang et al (2002) is based laboratory results (Ishihara and Yoshimine, 1992) to estimate liquefaction induced volumetric strains for sandy and silty soils, as shown on Figure 6. The procedure can be illustrated using a CPT profile from the Marina District site in California. Figure 7 illustrates the major steps in the CPT-based liquefaction potential analysis and shows the profiles of measured CPT tip resistance q_c , sleeve friction f_s , soil behavior type index I_c , cyclic resistance ratio CRR & cyclic stress ratio CSR, and factor of safety against liquefaction FS, respectively. The data in Figures 7a and 7b can be



directly obtained from the CPT sounding.

Figure 6. Relationship between post-liquefaction volumetric strain and equivalent clean sand normalized CPT tip resistance for different factors of safety (FS). (After Zhang et al., 2002)

Figures 7c, 7d and 7e show the results calculated based on the Robertson and Wride procedure shown in Figure 4. Note that, according to Robertson and Wride's approach, CRR is not calculated when the soil behavior type index is greater than 2.6. These soils are assumed to be non-liquefiable in Robertson and Wride's approach.

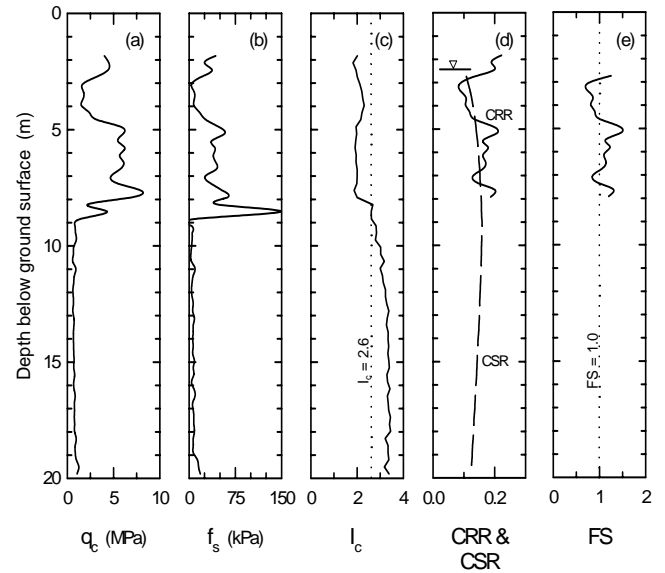


Figure 7. Example plots illustrating the major procedures in performing liquefaction potential analysis using the CPT based Robertson and Wride's (1998) method. (After Zhang et al., 2002)

The four key plots for estimating liquefaction induced ground settlements by the CPT-based method are presented in Figure 8. Figures 8a to 8d show the profiles of equivalent clean sand normalized tip resistance $(q_{c1N})_{cs}$, factor of safety FS, post-liquefaction volumetric strain ε_v , and liquefaction induced ground settlement S , respectively. Data in Figures 8a and 8b are from the liquefaction potential analysis. Data in Figure 8c are calculated from the results presented by Ishihara and Yoshimine, (1992) and shown in Figure 6. The settlement shown in Figure 8d is obtained using Equation [10] and the volumetric strains from Figure 8c.

The method by Zhang et al (2002) was evaluated using liquefaction-induced ground settlements from the Marina District and Treasure Island case histories damaged by liquefaction during the 1989 Loma Prieta earthquake. Good agreement between the calculated and measured liquefaction-induced ground settlements was found. Although further evaluations of the method are required with future case history data from different earthquakes and ground conditions, as they become available, it is suggested that the CPT-based method may be used to estimate liquefaction-induced settlements for low to medium risk projects and also provide preliminary estimates for higher risk projects.

6 EFFECTS OF OTHER MAJOR FACTORS ON CALCULATED SETTLEMENTS

6.1 Maximum surface acceleration

The amplification of earthquake motions is a complex process and is dependent on soil properties, thickness, frequency content of motions and local geological settings. For a given earthquake and geological setting, the amplification increases with the increase of soil compressibility and with soil thickness. Maximum surface acceleration at a site is one important parameter used in evaluating liquefaction potential of sandy soils. However, its determination is difficult without recorded accelerographs for a given earthquake because it likely varies with soil stratigraphy, soil properties, earthquake properties, the relative location of the site to the epicenter and even ground geometry. Ground response analysis may help to solve the problem but still leave some uncertainty in the results. Zhang et al. (2002) illustrated the importance of maximum surface acceleration and showed that calculated settlements are not linearly proportional to maximum surface acceleration beyond certain values since the calculated volumetric strains reach limiting values (Fig. 6). Using the Zhang et al (2002) approach it is possible to calculate settlements as a function of surface acceleration as a means to evaluate the sensitivity of the approach to the design earthquake.

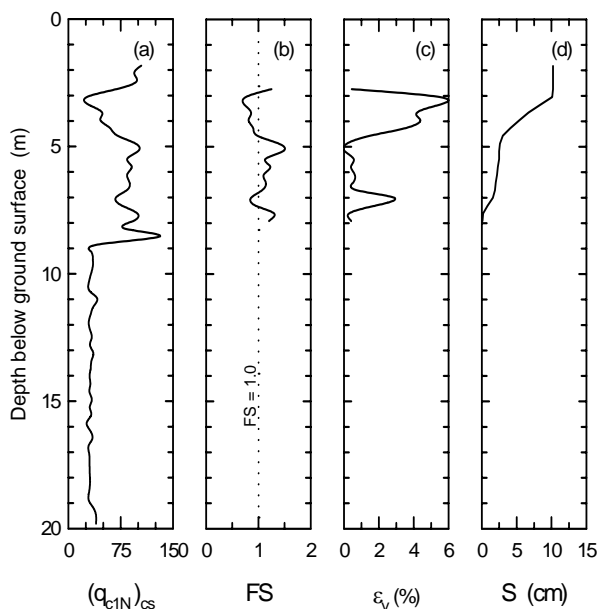


Figure 8. Example plots illustrating the major procedures in estimating liquefaction-induced ground settlements using the Zhang et al (2002) CPT based method.

6.2 Fines content or mean grain size

Although there are many practical situations where liquefaction settlements need to be estimated for sands with little silt to silty-sands, the volumetric strains shown in Figure 6 are applicable to saturated clean sands only. It is therefore necessary to consider the effects of fines content on post-liquefaction volumetric strains and liquefaction potential.

Volumetric strains tend to increase with increasing mean grain size at a given relative density (Lee and Albaisa 1974). Since increasing the fines content of a sand will result in a decrease of the mean grain size, it is postulated that post-liquefaction volumetric strains would decrease with increasing fines content in sands at a given relative density.

Silty sands have been found to be considerably less vulnerable to liquefaction than clean sands with similar SPT blow-counts (Iwasaki et al. 1978; Tatsuoka et al. 1980; Tokimatsu and Yoshimi 1981; Zhou 1981; et al.). Consequently, modification factors to SPT blow-counts or cyclic resistance ratio for sands with different fines contents or mean grain sizes had been widely used in liquefaction potential analyses (Seed and Idriss 1982; Robertson and Campanella 1985; Seed et al. 1985; Robertson and Wride 1998).

Zhang et al (2002) used the equivalent clean sand normalized CPT tip resistance ($(q_{c1N})_{cs}$) to account for the effects of sand grain characteristics and apparent fines content on CRR. $(q_{c1N})_{cs}$ is also used to estimate post-liquefaction volumetric strains for sands with fines. This approach assumes that both the liquefaction resistance and post-liquefaction deformations of silty sandy soils can be quantified using the same method and formulas as for clean sands provided that the equivalent clean sand normalized cone penetration resistance, $(q_{c1N})_{cs}$, is used. This implies that no further modification is required for the effects of fines content or mean grain size if $(q_{c1N})_{cs}$ is used to estimate the liquefaction induced settlements of sandy soils including silty sands. Because $(q_{c1N})_{cs}$ will increase with increase of fines content with sands for a given cone tip resistance, the calculated post-liquefaction volumetric strains will decrease with increase of fines content for a given factor of safety. This approach appears to indirectly account partially or wholly for the effect of grain characteristics on post-liquefaction volumetric strains and provides the same trend as observed by Lee and Albaisa (1974).

6.3 Transitional zone or thin sandy soil layers

It is recognized that transitional zones between soft clay layers and stiff sandy soil layers influence the calculated liquefaction-induced settlements. However, the influence of the transitional zones on calculated $(q_{c1N})_{cs}$, and FS has been partially counteracted implicitly in the Robertson and Wride method. Generally, the measured tip resistance in a sandy soil layer close to a soft soil layer (usually a clayey soil layer) is smaller than the “actual” tip resistance (if no layer interface existed) and the resultant friction ratio is greater than the “actual” friction ratio due to the influence of the soft soil layer. As a result, the calculated value of I_c will increase, and therefore the correction factor K_c , $(q_{c1N})_{cs}$, and FS will increase as well. $(q_{c1N})_{cs}$ and FS may be close to the “true” values in the same sandy soil layer that is not influenced by the adjacent soft soil layer. Therefore, the calculated ground settlements would be close the “actual” values because of this implicit correction incorporated within the Robertson and Wride method.

Zhang et al. (2001) took no correction in an attempt to quantify the influences of both the transitional zones and thin sandy layers on the tip resistance, yet achieved good agreement with the limited case history results. Making no correction for transitional zones and thin layers is conservative when estimating liquefaction potential and liquefaction related deformations. Further investigation is required to quantify the influence of transitional zones or thin sandy soil layers on calculated FS and liquefaction-induced ground settlements.

6.4 Three dimensional distribution of liquefied soil layers

The thickness, depth and lateral distribution of liquefied layers will play an important role on ground surface settlements. Liquefaction of a relatively thick but deep sandy soil (see Figure 9a) may have minimal effect on the performance of an overlying structure founded on shallow foundations. However, liquefaction of a near surface thin layer of soil (Figure 9b) may have major implications on the performance of the same structure.

Ishihara (1993) provided some guidance on the effect of thickness and depth to the liquefied layer on potential settlements that may be reasonable provided that the site is not susceptible to ground oscillation or lateral spread. Gilstrap (1998) concluded that Ishihara’s relationship for predicting surface effects may be oversimplified. As well, the application of Ishihara’s criteria in practice for cases with multiple liquefied layers (Figure 9c) is not clear.

The lateral extent of liquefied layers may also have an effect on ground surface settlements. A small locally liquefied soil zone with limited lateral extent (Figure 9d) would have limited extent of surface manifestation than that for a horizontally extensive liquefied soil zone with the same soil properties and vertical distribution of the liquefied layer. On the other hand, the locally liquefied soil zone may be more damaging to the engineered structures and facilities due to the potential large differential settlements. However, no quantitative study has been reported for the effect of lateral extent of liquefied layers on ground surface settlements.

Neglecting the effect of three-dimensional distribution of liquefied layers on ground surface settlements may result in over-estimating liquefaction-induced ground settlements for some sites. Engineering judgement is needed to avoid an overly conservative design. Case histories from previous earthquakes have indicated that little or no surface manifestation was observed for cases where the depth from ground surface to the top of the liquefied layer was greater than 20 m. Care is required to detect local zones of soil that may liquefy and to estimate the potential differential settlements that may occur.

6.5 Factor K_c

Robertson and Wride (1998) recommended the factor K_c be set equal to 1.0 rather than using K_c of 1.0 to 2.14 when the CPT data plot in the zone defined by $1.64 < I_c < 2.36$ and $F < 0.5\%$ to avoid confusion of very loose clean sands with denser sands containing fines. However, if the CPT data of a dense sand with fines plots in the zone ($1.64 < I_c < 2.36$ and $F < 0.5\%$), the calculated $(q_{c1N})_{cs}$ value for the dense sand could be reduced by one-half. Although this recommendation is conservative for evaluating liquefaction potential of sandy soils, it may result in over-estimating liquefaction-induced ground settlements for sites with denser sands containing fines that fit in that zone. This seems to be true for some of the CPT soundings in the two case histories studied by Zhang et al (2002). For example, based on soil profiles, CPT profiles, and engineering judgment, a portion of the soil that should have been assessed as dense sand containing fines, was classified as very loose clean sand with K_c equal to 1.0.

Zhang et al (2002) showed that when the settlements for the two case histories were recalculated without following the recommendation of K_c equal to 1.0 for $1.64 < I_c < 2.36$ and $F < 0.5\%$, there was almost no effect for the western and central parts of Marina District and only small (up to 14%) effects for Treasure Island. However the

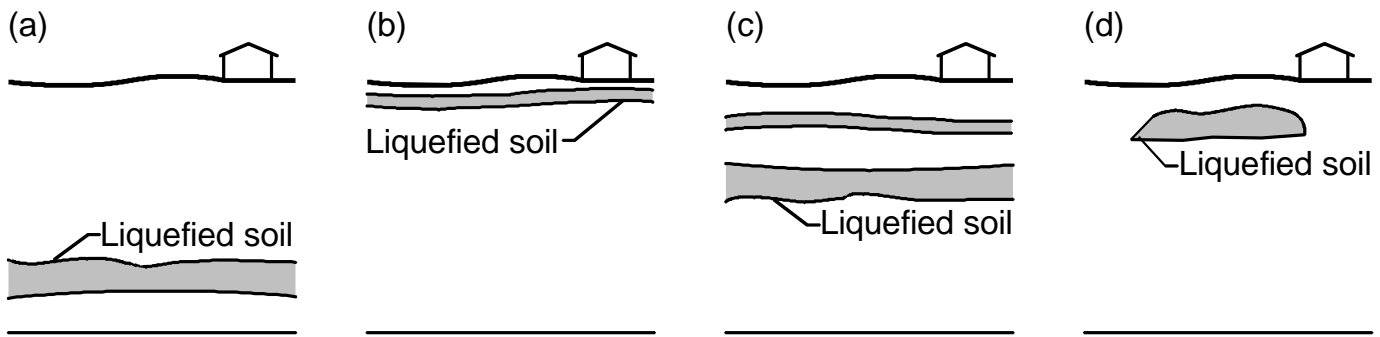


Figure 9. Four hypothetical cases showing importance of three-dimensional distribution of liquefied layers.

calculated settlements for the eastern part of Marina District were reduced by a factor of about 2 without the recommendation for K_c . The effect of this recommendation on calculated ground settlements depends on the amount of the soils that fit in the zone defined by $1.64 < I_c < 2.36$ and $F < 0.5\%$ within a soil profile for a site studied. If a large amount of the soils fit in this zone, the effect could be more significant than that for the two case history sites studied above. Soil sampling is therefore recommended to clarify soil properties for sites where a large amount of soil plots in the zone $1.64 < I_c < 2.36$ and $F < 0.5\%$.

6.6 Cutoff of I_c equal to 2.6

A cutoff of I_c equal to 2.6 is used to distinguish sandy and silty soils from clayey soils, which are believed to be non-liquefiable (Robertson and Wride, 1998). Gilstrap (1998) concluded that the I_c cutoff of 2.6 recommended by Robertson and Wride (1998) is generally reliable for identifying clayey soils, but noticed that 20% to 50% of the samples with I_c between 2.4 to 2.6 were classified as clayey soils based on index tests. This implies that the cutoff of I_c equal to 2.6 appears slightly conservative.

Zhang et al (2002) investigated the sensitivity of the calculated settlements to this cutoff for the two case histories using a cutoff of I_c equal to 2.5. The calculated settlements with the cutoff of I_c equal to 2.5 were slightly smaller than with the cutoff of 2.6. For the two cases, only a small portion of the soil in the profiles had I_c ranging from 2.5 to 2.6, thus the use of a cutoff of I_c equal to 2.6 does not greatly overestimate the settlements.

Neglecting the influence of the recommendation for K_c and the cutoff line of I_c equal to 2.6 on the calculated ground settlements is conservative. However, soil sampling is recommended to avoid unnecessary overestimation of liquefaction-induced ground settlements for some sites where a large amount of the soils have a calculated I_c close

to 2.6 or/and fit in the zone defined by $1.64 < I_c < 2.36$ and $F < 0.5\%$.

7 LIQUEFACTION INDUCED LATERAL DISPLACEMENTS

Generally, liquefaction-induced ground failures include flow slides, lateral spreads, ground settlements, ground oscillation, and sand boils. Lateral spreads are the pervasive types of liquefaction-induced ground failures for gentle slopes or for nearly level (or gently inclined) ground with a free face (e.g., river banks, road cuts).

Several methods have been proposed to estimate liquefaction-induced lateral ground displacements including numerical models, laboratory tests, and field-test-based methods. Challenges associated with sampling loose sandy soils limit the applications of numerical and laboratory testing approaches in routine practice. Field-test-based methods are likely best suited to provide simple direct methods to estimate liquefaction-induced ground deformations for low- to medium-risk projects and to provide preliminary estimates for high-risk projects.

One-g shake table tests have been conducted to investigate the mechanisms of liquefaction-induced ground lateral spreads. These tests support the hypothesis that lateral spreads result from distributed residual shear strains throughout the liquefied layers. The residual shear strains in liquefied layers are primarily a function of: (a) maximum cyclic shear strains γ_{max} , and (b) biased insitu static shear stresses. In this paper, γ_{max} refers to the maximum amplitude of cyclic shear strains that are induced during undrained cyclic loading for a saturated sandy soil without biased static shear stresses in the direction of cyclic loading. Biased insitu static shear stresses are mainly controlled by ground geometry at the site (e.g., ground slope, free face height, and the distance to a free face). The thickness of liquefied layers will

also influence the magnitude of lateral displacements, with greater lateral displacements for thicker liquefied layers. Both γ_{\max} and the thickness of liquefied layers are affected by soil properties and earthquake characteristics.

Zhang et al (2004) suggested a semi-empirical method based on CPT results to estimate the lateral displacement using the combined results from laboratory tests with case history data from previous earthquakes. The method captures the mechanisms of liquefaction-induced lateral spreads and characterizes the major factors controlling lateral displacements. Application of the method is simple and can be applied with only a few calculations following the CPT-based liquefaction potential analysis. The approach may be suitable to estimate the magnitude of lateral displacements associated with liquefaction-induced lateral spread for gently sloping (or level) ground with or without a free face for low to medium-risk projects, or to provide preliminary estimates for higher risk projects.

The Zhang et al (2004) method uses the laboratory results presented by Ishihara and Yoshimine (1992) to estimate the maximum shear strains, γ_{\max} , as shown on Figure 10. Zhang et al (2004) used the correlation between D_r and normalized cone tip resistance (q_{c1N}) suggested by Tatsuoka et al. (1990):

$$D_r = -85 + 76 \log(q_{c1N}) \quad (q_{c1N} \leq 200) \quad [11]$$

Where: q_{c1N} is the normalized CPT tip resistance corrected for effective overburden stresses corresponding to 100 kPa (Robertson and Wride, 1998).

This correlation provides slightly smaller and more conservative estimates of relative density than the correlation by Jamiolkowski et al. (1985) when q_{c1N} is less than about 100.

Integrating the calculated γ_{\max} values with depth will produce a value that is defined as the lateral displacement index, (LDI):

$$LDI = \int_0^{Z_{\max}} \gamma_{\max} dz \quad [12]$$

where Z_{\max} is the maximum depth below all the potential liquefiable layers with a calculated FS < 2.0.

Using case history results and ground geometric parameters to characterize the ground geometry, the lateral displacement (LD) can be estimated.

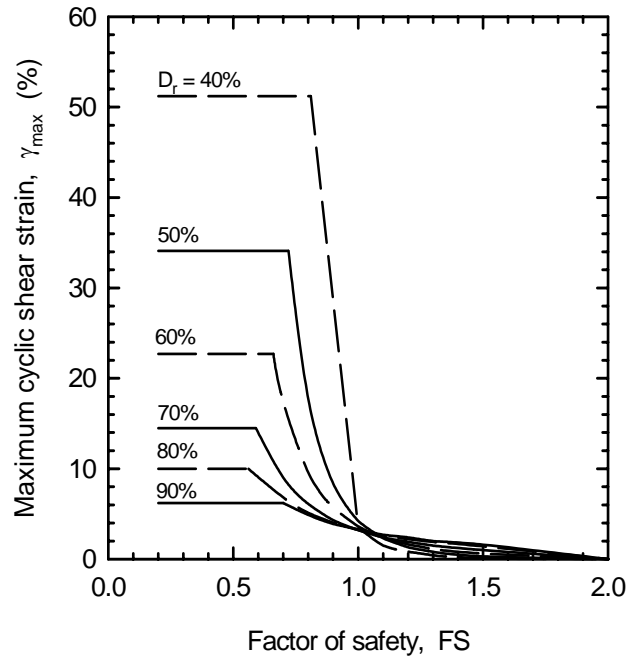


Figure 10. Relationship between maximum cyclic shear strain and factor of safety for different relative densities D_r for clean sands (after Zhang et al., 2004).

For gently sloping ground without a free-face; Zhang et al (2004) suggested the following relationship based on the available case histories;

$$\frac{LD}{LDI} = S + 0.2 \quad (\text{for } 0.2\% < S < 3.5\%) \quad [13]$$

Where: S is the ground slope as a percentage.

For level ground conditions with a free-face; Zhang et al (2004) suggested the following relationship based on the available case histories:

$$\frac{LD}{LDI} = 6 \cdot \left(\frac{L}{H} \right)^{-0.8} \quad (\text{for } 4 < L/H < 40) \quad [14]$$

Where: L is the horizontal distance from the toe of a free-face,

H is the height of the free-face.

Level ground is taken as ground with a slope less than 0.15%.

The Zhang et al (2004) approach is recommended for use within the ranges of earthquake properties, moment magnitude (M_w) between 6.4 and 9.2, and, peak surface acceleration (a_{\max}) between 0.19g and 0.60 g, and free face heights less than 18 m. The case history data used for developing the approach, especially for gently sloping

ground without a free face, were dominantly from two Japanese case histories associated with the 1964 Niigata and 1983 Nihonkai-Chubu earthquakes, where the liquefied soils were mainly clean sand only. The values for the geometric parameters used in developing the approach were within limited ranges, as specified in Equations [13] and [14]. It is recommended that the approach not be used when the values of the geometric parameters go beyond the specified ranges.

The approach by Zhang et al (2004) is suitable to estimate the magnitude of lateral displacements associated with liquefaction-induced lateral spread for gently sloping (or level) ground with or without a free face for low to medium-risk projects, or to provide preliminary estimates for higher risk projects. Given the complexity of liquefaction-induced lateral spreads, considerable variations in magnitude and distribution of lateral displacements are expected. Generally, the calculated lateral displacements using the proposed approach for the available case histories showed variations between 50% and 200% of measured values. The accuracy of “measured” lateral displacements for most case histories is about ± 0.1 to ± 1.92 m. Therefore, it is unrealistic to expect the accuracy of estimated lateral displacements be within ± 0.1 m. The reliability of the proposed approach can be fully evaluated only over time with more available case histories.

The approach by Zhang et al (2004) was developed using case history data with limited ranges of earthquake parameters, soil properties, and geometric parameters. Therefore, it is not recommended that the approach be applied for values of input parameters beyond the specified ranges. Engineering judgement and caution should be always exercised in applying the proposed approach and in interpreting the results. Additional new data are required to further evaluate and update the proposed approach.

8 FLOW LIQUEFACTION

When a soil is strain softening there is the potential for instability. The key response parameter required to estimate if a flow slide would occur is the minimum (residual or liquefied) undrained shear strength, S_{min} following strain softening. Methods have been suggested to estimate the minimum (liquefied) undrained shear strength of clean sands from penetration resistance based on case histories (Seed and Harder, 1990; Stark and Mesri, 1992). A recent re-evaluation of these case histories (Wride et al., 1998) has questioned the validity of the proposed correlation. Recent research has also

shown the importance of direction of loading on the minimum undrained shear strength of sands. The minimum undrained shear strength in triaxial compression (TC) loading is higher than that in simple shear (SS), which in turn, is larger than that in triaxial extension (TE). The difference is less as the sand becomes looser. Hence, the appropriate undrained shear strength to be used in a stability analyses will be a function of direction of loading. This has been recognized for some time in clay soils (Bjerrum, 1972).

The possibility of instability in undrained shear is also linked to the brittleness or sensitivity of the soil. Brittleness index (Bishop, 1967) is an index of the collapsibility of a strain softening soil when sheared undrained, which is defined as follows:

$$I_B = \frac{S_{peak} - S_{min}}{S_{peak}} \quad [15]$$

Where:

S_{peak} = the peak shear resistance prior to strain softening

S_{min} = the minimum undrained shear strength

A value of $I_B = 1$ indicates zero minimum undrained shear strength. If there is no strain softening then $I_B = 0$.

Figure 11 shows a link between the response characteristics of brittleness and minimum undrained strength ratio with only a small influence of direction of loading. When the minimum undrained strength ratio decreases, the brittleness increases. The sands are essentially non-brittle ($I_B = 0$) when the minimum undrained strength ratio (S_{min}/p') is greater than about 0.2 for TE, 0.25 for SS and 0.40 for TC. These values are similar to those observed for fine grained (clay) soils of low plasticity (Jamiolkowski et al., 1985). When the undrained strength ratio is less than about 0.1 the brittleness is usually high.

Yoshimine et al. (1998) proposed a relationship between normalized cone penetration resistance and the minimum undrained shear strength in simple shear loading for clean sands based on a combination of laboratory testing and case histories, as shown in Figure 12. The method suggested by Robertson and Wride (1998), can be used to calculate the equivalent clean sand normalized penetration resistance, $(q_{c1N})_{cs}$, which can then be used to estimate the minimum undrained shear strength ratio using Figure 12. The resulting values of minimum undrained shear strength ratio are approximate and apply primarily to young, normally consolidated, uncemented soils.

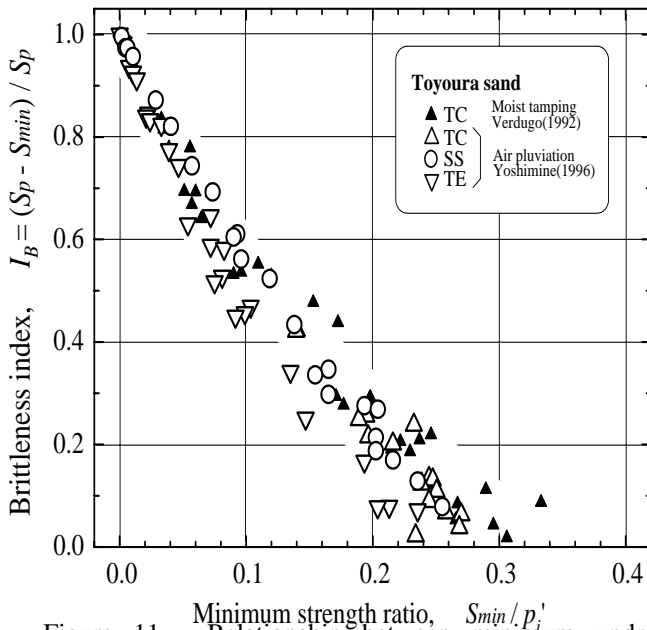


Figure 11. Relationship between minimum undrained strength ratio and brittleness index for clean sand (Yoshimine et al., 1998)

Sandy soils with angular grains and aged soils would likely have higher strengths. The actual value of s_{min} to be applied to any given problem will depend on the ground geometry, but in general, the simple shear direction of loading, $(s_{min})_{SS}$, represents a reasonable average value for most problems.

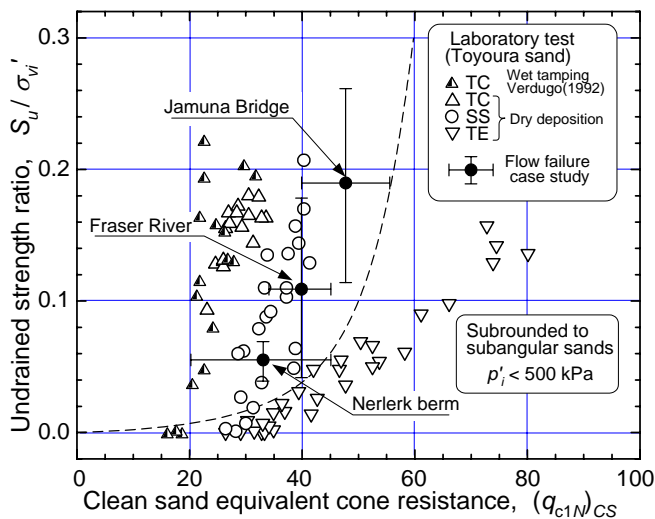


Figure 12. Undrained strength ratio from CPT for clean sand. (After Yoshimine et al., 1998).

Soils that have a minimum undrained shear strength ratio in simple shear of around 0.30 or

higher are generally not brittle. Soils that have a minimum undrained shear strength ratio of around 0.10 or less are often highly brittle. Hence, the value of $s_{u(min)}/\sigma'_{vo} = 0.10$ represents the approximate boundary between soils that can show significant strain softening in undrained simple shear and soils that are general not strain softening. For simple shear direction of loading, this boundary can be represented by a normalized clean sand equivalent CPT value of $(q_{c1N})_{cs} = 50$ (see Figure 12). Hence, a value of $(q_{c1N})_{cs} < 50$ can be used as an approximate criteria to estimate if a soil may be brittle and strain softening in undrained simple shear. If the soil is cohesionless (i.e. non-plastic, $I_c < 2.6$) the loss of strength could occur rapidly over small strains (brittle). If the soil is cohesive the loss of strength could occur more slowly, depending on the degree of sensitivity and plasticity of the soil. Highly sensitive clays (quick clays) can lose their strength rapidly resulting in flow slides. Less sensitive clays tend to deform gradually without a flow slide.

Olsen and Stark (2002) reviewed case histories of flow liquefaction and showed that there was no evidence of flow liquefaction where the mean normalized cone resistance (q_{c1N}) was greater than 65, although only two data points (out of 32) exceeded a value of 50. They also showed that when the normalized cone resistance was less than 50 the minimum (liquefied) shear strength ratio was less than 0.1. No case history had a back-calculated liquefied shear strength greater than 0.12. Only 7 case histories had measured CPT values, the remaining had values either converted from measured SPT, or had estimated CPT values. Olsen and Stark (2002) suggested an average relationship described by;

$$s_{u(LIQ)} / \sigma'_{vo} = 0.03 + 0.00143 (q_{c1N}) \pm 0.03 \quad [16]$$

$$\text{for } q_{c1N} < 65$$

The data presented by Olsen and Stark (2002) made no adjustment for fines content, although the case histories indicated a range in fines contents from 0 to 100%.

The approach suggested by Yoshimine et al. (1998) tends to produce conservative low values compared to the Olsen and Stark (2002) method. Both methods are appropriate for young unconsolidated, normally consolidated soils where the vertical effective stress is less than about 300 kPa and $I_c \leq 2.6$. In sandy soils where the sand grains are angular the methods may under predict the undrained shear strength. Where the in-situ effective stress is greater than 300 kPa, the minimum undrained shear strength could be smaller depend-

ing on the compressibility of the soil. Soils that fall in the lower left region of the CPT soil behavior chart ($F < 1\%$, $I_c > 2.6$) may be sensitive and may be susceptible to both cyclic and flow liquefaction depending on soil plasticity, sensitivity (brittleness). Clay soils, where $I_c > 2.6$ and $F > 1\%$, are generally non-liquefiable. For high-risk projects, it is advisable to obtain samples to evaluate their liquefaction (strain softening) potential using other criteria.

9 REPRESENTATIVE VALUES

When evaluating the potential for flow liquefaction, there is little guidance given on what value of penetration resistance can be taken as representative of the deposit. In the SPT and CPT based methods for cyclic liquefaction suggested by the NCEER Workshop (Youd et al., 2001), the average values were taken from the case histories to develop the method. However, the CPT-based approach is generally applied using all the continuous CPT data. In general, if all values of the measured penetration resistance are used with a relationship that was based on average values, the resulting design will generally be somewhat conservative.

Seed and Harder (1990), Stark and Mesri (1992) and Olson and Stark (2002) used average values from case histories to develop the relationship between either $(N_1)_{60}$ or q_{c1N} and minimum (liquefied) undrained shear strength to estimate the potential for flow liquefaction. Wride et al. (1998) argued that the minimum value of penetration resistance should be more appropriate. A disadvantage of defining a criteria based on minimum values (especially for the SPT) is the uncertainty that the measured values represent the minimum. In practice, a lower bound relationship is often applied to all measured penetration resistance values. Popescue et al. (1997) suggested that the 20-percentile value would be appropriate as the representative value for cyclic liquefaction. The 20-percentile value is defined as the value at which 20 percent of the measured values are smaller (i.e. 80 percent are larger).

Olsen and Stark (2002) used mean values of penetration resistance because most flow failure case histories had insufficient test results to reasonably estimate 20-percentile values. They suggest that if minimum values of penetration resistance are used for design in conjunction with their empirical correlation (equation 16), engineers should consider selecting a liquefied strength ratio greater than the average relationship (i.e. the upper bound values). The boundary suggested by Yo-

shimine et al. (1998) is essentially a lower bound relationship that applies to mean values and appears to be more conservative than the relationship suggested by Olsen and Stark (2002).

In the authors' opinion, the mean value is likely the more representative value for any given deposit for the evaluation of flow liquefaction potential based on the criteria of $(q_{c1N})_{cs} = 50$, although factors such as, ground geometry, soil profile and the probability of a triggering event can influence the representative value. Olsen and Stark (2002) suggest using mean values and the average relationship (equation 16). If the mean value of the CPT $(q_{c1N})_{cs} > 50$ than flow liquefaction is unlikely. Olsen and Stark (2002) suggest that to incorporate a strength ratio in a post-triggering stability analysis, a liquefied soil layer can be separated into a number of sublayers of equal σ'_{vo} (stress contours) and (or) equal penetration resistance (penetration contours). For example, each vertical effective stress contour would have an equal value of $s_u (LIQ)$, and $s_u (LIQ)$ would increase as σ'_{vo} contours increase.

10 SUMMARY

For low-risk, small-scale projects, the potential for cyclic liquefaction can be estimated using penetration tests such as the CPT. The CPT is generally more repeatable than the SPT and is the preferred test, where possible. The CPT provides continuous profiles of penetration resistance, which are useful for identifying soil stratigraphy and for providing continuous profiles of estimated cyclic resistance ratio (CRR). Corrections are required to both the SPT and CPT results for grain characteristics, such as fines content and plasticity. For the CPT, these corrections are best expressed as a function of soil behavior type, I_c , which is affected by the full range of grain characteristics.

For medium- to high-risk projects, the CPT can be useful for providing a preliminary estimate of liquefaction potential in sandy soils. For higher risk projects, and in regions where there is little previous CPT experience, it is also preferred practice to drill sufficient boreholes with selective sampling adjacent to the CPT soundings to verify various soil types encountered and to perform index testing on disturbed samples. A procedure has been described to correct the measured cone resistance for grain characteristics based on the CPT soil behavior type, I_c . The corrections are approximate, since the CPT responds to many factors affecting soil behavior. Expressing the corrections in terms of soil behavior index is the preferred method of incorporating the effects of various grain characteristics, more than just fines content.

When possible, it is recommended that the corrections be evaluated and modified to suit a specific site and project. However, for small-scale, low-risk projects and in the initial screening process for higher risk projects, the suggested general corrections provide a useful conservative guide and provide continuous profiles that capture the full detail of the soil profile.

It is also useful to evaluate CRR using more than one method. For example, the seismic CPT (SCPT) can provide a useful technique to independently evaluate liquefaction potential, since it measures both the usual CPT parameters, as well as shear wave velocity, within the same soil profile. The CPT provides detailed profiles of cone resistance, but the penetration resistance is sensitive to grain characteristics, such as fines content, soil plasticity and mineralogy, and hence corrections are required. The seismic part of the SCPT provides a shear wave velocity profile typically averaged over 1m intervals and, therefore contains less detail than the cone tip resistance profile. However, shear wave velocity is less influenced by grain characteristics and few or no corrections are required (Andrus and Stokoe, 1998). Shear wave velocity should be measured with care to provide the most accurate results, since the estimated CRR is sensitive to small changes in shear wave velocity. There should be consistency in the liquefaction evaluation using either method. If the two methods provide different predictions of CRR profiles, samples should be obtained to evaluate the grain characteristics of the soil. Differences between the shear wave velocity and penetration resistance methods can be caused by aging, cementation and grain compressibility (Lunne et al., 1997).

A key advantage of the integrated CPT method is that the algorithms can easily be incorporated into a spreadsheet or software, as illustrated by the Moss Landing example. The result is a straightforward method for analysing the entire CPT profile in a continuous manner. This provides a useful tool for the engineer to review the potential for cyclic liquefaction across a site using engineering judgement.

An extension to the CPT-based method to evaluate liquefaction potential was suggested by Zhang et al (2002 and 2004) and allows estimates of vertical settlements and lateral spread deformations to be made using the continuous CPT profile.

The method by Zhang et al (2002) to estimate post-earthquake vertical settlements was evaluated using liquefaction-induced ground settlements from the Marina District and Treasure Island case histories damaged by liquefaction during the 1989 Loma Prieta earthquake. Good agreement between the calculated and measured liquefaction-induced ground settlements was found. Although further evaluations of the method are required with future

case history data from different earthquakes and ground conditions, as they become available, it is suggested that the CPT-based method may be used to estimate liquefaction-induced settlements for low to medium risk projects and also provide preliminary estimates for higher risk projects.

The method by Zhang et al (2004) to estimate lateral displacements was developed using case history data with limited ranges of earthquake parameters, soil properties, and geometric parameters. Therefore, it is not recommended that the approach be applied for values of input parameters beyond the specified ranges. Engineering judgement and caution should always be exercised in applying the proposed approach and in interpreting the results. Additional new data are required to further evaluate and update the proposed approach.

Soils that have a minimum undrained shear strength ratio of around 0.10 or less are often highly brittle. Hence, the value of $s_{u(\min)}/\sigma'_{vo} = 0.10$ represents the approximate boundary between soils that can show significant strain softening in undrained simple shear and soils that are general not strain softening. Research has clearly shown that the undrained shear strength of soils is usually a function of direction of loading, with undrained shear strengths in compression loading often being higher than those in simple shear and triaxial extension. The resulting average minimum undrained shear strength is therefore a function of the slope geometry. Although all projects should be evaluated based on their actual geometry, often the average undrained shear strength is close to that in simple shear loading, which is consistent with the observations made by Bjerrum (1972) for slopes and embankments in clays. For simple shear direction of loading, this boundary can be represented by a normalized clean sand equivalent CPT value of $(q_{c1N})_{cs} = 50$. Hence, a limit of $(q_{c1N})_{cs} < 50$ can be used as an approximate criteria to estimate if a soil may be brittle and strain softening in undrained simple shear. The recent review of flow failure case histories by Olsen and Stark (2002) confirm this value. If the soil is cohesionless (i.e. non-plastic, $I_c < 2.6$) the loss of strength could occur rapidly over small strains (brittle). If the soil is cohesive the loss of strength could occur more slowly, depending on the degree of sensitivity and plasticity of the soil. Highly sensitive clays (quick clays) can lose their strength rapidly resulting in flow slides. Less sensitive clays tend to deform gradually without a flow slide.

Sands that have angular grains may have a minimum (liquefied) undrained strength ratio higher than predicted using the suggested CPT methods by Yoshimine et al (1998) and Olsen and Stark (2002). Aged soils (age > 1,000 years) may also be somewhat stronger. For high-risk projects,

the proposed CPT criteria (based on $(q_{c1N})_{cs} < 50$) provides a useful screening technique to identify potentially critical zones where flow liquefaction may be possible. For low risk projects, the proposed CPT methods will generally provide a conservative estimate of the minimum undrained shear strength ratio in simple shear loading. The proposed relationship conservatively estimates the minimum (liquefied) undrained shear strength ratio for a soil structure that contains extensive amounts of loose sandy soils with impeded drainage, such as thick deposits of loose interbedded sands and silts. In soil structures where drainage and consolidation of the liquefied layer can occur during and immediately after the earthquake, higher values of undrained shear strength will likely exist. Such conditions may exist in a thin deposit with free drainage to the ground surface or a deposit interbedded with extensive pervious gravel layers.

ACKNOWLEDGEMENTS

This paper is a summary of many years of research that have involved many colleagues and graduate students as well as support by the Natural Science and Engineering Research Council of Canada (NSERC).

REFERENCES

- Andrus, R.D., and Stokoe, K.H. 1998. Guidelines for evaluation of liquefaction resistance using shear wave velocity. Proceedings of the NCEER (National Center for Earthquake Engineering Research) workshop on evaluation of liquefaction resistance of soils, Salt Lake City, Utah, January 1996, T.L. Youd and I.M. Idriss (eds.), NCEER-97-0022, 89-128.
- Bishop, A.W. 1967. Progressive failure – with special reference to the mechanism causing it. Panel discussion. Proceedings of the Geotechnical Conference, Oslo, Norway, 2: 142-150.
- Bjerrum, L., 1972, Embankments on soft ground. Proceedings of Specialty Conference on Performance of Earth and Earth-supported structures, Lafayette, Indiana, 2: 1-54.
- Bartlett, S.F., and Youd, T.L. 1995. Empirical prediction of liquefaction-induced lateral spread. Journal of Geotechnical Engineering, ASCE, **121**(4): 316-328.
- Boulanger, R.W., Mejia, L.H., and Idriss, I.M. 1997. Liquefaction at Moss Landing during Loma Prieta earthquake. Journal of Geotechnical and Geoenvironmental Engineering, ASCE, **123**(5): 453-468.
- Ishihara, K., 1993. Liquefaction and flow failure during earthquakes. 33rd Rankine Lecture, Geotechnique, 43(3): 349-415.
- Ishihara, K., and Yoshimine, M. 1992. Evaluation of settlements in sand deposits following liquefaction during earthquakes. Soils and Foundations, **32**(1): 173-188.
- Iwasaki, T., Tatsuoka, F., Tokida, K., and Yasuda, S. 1978. A practical method for assessing soil liquefaction potential based on case studies at various sites in Japan. Proceeding of the Second International Conference of Microzonation, San Francisco, CA, Vol. 2, pp.885-896.
- Jamiolkowski, M., Ladd, C.C., Germaine, J.T., and Lancellotta, R. 1985. New developments in field and laboratory testing of soils. In Proceedings of the Eleventh International Conference on Soil Mechanics and Foundation Engineering, San Francisco, 12-16 August, Vol. 1, pp. 57-153.
- Juang, C. H., Chen, C. J., and Tien, Y. M. 1999a. Appraising CPT-based liquefaction resistance evaluation methods -- artificial neural network approach. Canadian Geotechnical Journal, **36**(3): 443-454.
- Juang, C. H., Rosowsky, D. V., and Tang, W. H. 1999b. Reliability-based method for assessing liquefaction potential of soils. Journal of Geotechnical and Geoenvironmental Engineering, ASCE, **125**(8): 684-689.
- Lee, K. L., and Albaisa, A. 1974. Earthquake induced settlements in saturated sands. Journal of Geotechnical Engineering, ASCE, **100**(GT4): 387-406.
- NCEER 1997. Proceeding of the NCEER Workshop on Evaluation of Liquefaction Resistance of Soils, Edited by Youd, T. L., and Idriss, I. M., Technical Report NCEER-97-0022, Salt Lake City, Utah, Decemeber 31, 1997.
- Olsen, R.S., and Malone, P.G. 1988. Soil classification and site characterization using the cone penetrometer test. Penetration Testing 1988, ISOPT-1, Edited by De Ruiter, Balkema, Rotterdam, 2: 887-893.
- Olsen, S.M. and Stark, T.D., 2002. Liquefied Strength ratio from liquefaction flow failure case histories. Canadian Geotechnical Journal, 39: 629-647
- Popescu, R., Prevost, J.H., and Deodatis, G., 1997. Effects of spacial variability on soil liquefaction: some design recommendations. Geotechnique, 47(5): 1019-1036
- Robertson, P.K., 1990. Soil Classification using the CPT. Canadian Geotechnical Journal. 27(1),151-158.
- Robertson, P.K., and Wride C.E. 1998. Evaluating cyclic liquefaction potential using the CPT. Canadian Geotechnical Journal, **35**(3): 442-459.

- Robertson, P. K., and Campanella, R. G. 1985. Liquefaction potential of sands using the cone penetration test. *Journal of Geotechnical Engineering*, ASCE, **22**(3): 298-307.
- Seed, H.B. 1979. Soil liquefaction and cyclic mobility evaluation for level ground during earthquakes. *Journal of Geotechnical Engineering Division*, ASCE, **105**(GT2): 201-255.
- Seed, H. B., and Idriss, I. M. 1971. Simplified procedure for evaluation soil liquefaction potential. *Journal of the Soil Mechanics and Foundations Division*, ASCE, **97**(SM9): 1249-1273.
- Seed, H. B., and Idriss, I. M. 1982. Ground motions and soil liquefaction during earthquakes. *Earthquake Engineering Research Institute*, p.134.
- Seed, H. B., Tokimatsu, K., Harder, L. F., and Chung, R. M. 1985. Influence of SPT procedures in soil liquefaction resistance evaluations. *Journal of Geotechnical Engineering*, ASCE, **111**(12): 1425-1440.
- Seed, R. B., and Harder, L. F. 1990. SPT-based analysis of cyclic pore pressure generation and undrained residual strength. *Proceedings H. B. Seed Memorial Symp.*, Vol. 2, BiTech Publishers, Vancouver, BC, May, pp.351-376.
- Stark, T.D., and Mesri, G.M., 1992. Undrained shear strength of liquefied sands for stability analysis. *Journal of Geotechnical Engineering*. ASCE, **118** (11): 1727-1747.
- Tatsuoka, F., Iwasaki, T., Tokida, K., Yasuda, S., Hirose, M., Imai, T., and Kon-no, M. 1980. Standard penetration tests and soil liquefaction potential evaluation. *Soils and Foundations*, JSSMFE, **20**(4): 95-111.
- Tokimatsu, K. and Yoshimi, Y. 1981. Field correlation of soil liquefaction with SPT and grain size. *Proceedings of Eight World Conference on Earthquake Engineering*, San Francisco, CA, 95-102.
- Yoshimine, M., Robertson, P.K., and Wride, C.E., 1998, Undrained shear strength of clean sands, Accepted for publication in the *Canadian Geotechnical Journal*.
- Wride, C.E., McRoberts, E.C. and Robertson, P.K., 1998. Reconsideration of Case Histories for Estimating Undrained Shear strength in Sandy soils. Accepted for publication in the *Canadian Geotechnical Journal*.
- Youd, T.L., Idriss, I.M, Andrus, R.D., Arango, I., Castro, G., Christian, J.T., Dobry, R., Finn, W.D.L., Harder, L.F., Hynes, M.E., Ishihara, K., Koester, J.P., Liao, S.S.C., Marcuson, W.F., Martin, G.R., Mitchell, J.K., Moriwaki, Y., Power, M.S., Robertson, P.K., Seed, R.B., Stokoe, K.H. 2001. Liquefaction resistance of soils: summary report from the 1996 NCEER and 1998 NCEER/NSF Workshops on evaluation of liquefaction resistance of soils. *Journal of Geotechnical and Geoenvironmental Engineering*, **127**(4): 297 – 313.
- Zhang, G., Robertson, P.K. and Brachman, R.W.I, 2002. Estimating liquefaction-induced ground settlements from CPT for level ground. *Canadian Geotechnical Journal*, **39**: 1168-1180
- Zhang, G., Robertson, P.K. and Brachman, R.W.I, 2004. Estimating liquefaction-induced lateral displacements using the SPT or CPT. *Journal of Geotechnical and Geoenvironmental Engineering*.
- Zhou, S. G. 1981. Influence of fines on evaluating liquefaction of sand by CPT. *Proceedings of International Conference on Recent Advances in Geotechnical Earthquake Engineering and Soil Dynamics*, St. Louis, MO, **1**, 167-172.